Engineering with Computers (2018) 34:339–345
https://doi.org/10.1007/s00366-017-0544-8

ORIGINAL ARTICLE

Developing GPR model for forecasting the rock fragmentation in surface mines

Wei Gao[1] · Masoud Karbasi[2] · Mahdi Hasanipanah[3] · Xun Zhang[4] · Jia Guo[5]

Received: 6 August 2017 / Accepted: 10 November 2017 / Published online: 20 November 2017

Abstract
Blasting operation is an economical and common method for rock fragmentation in civil construction works, surface and underground mines. The aim of this study is to present an accurate model for predicting the rock fragmentation (D_{80}) induced by blasting in Shur river dam region, Iran, through Gaussian process regression (GPR). For this aim, 72 blasting events were investigated and the values of six parameters, i.e. burden, spacing, stemming, powder factor, charge used per delay and D_{80} were measured. Firstly, 80% of the total data (58 datasets) were assigned to train the GPR, whereas the remaining 14 datasets were assigned to test the constructed GPR model. In GPR modeling, 5 different kernels, i.e. squared exponential, exponential, matern32, matern52 and rational quadratic, were employed. The proposed GPR models were then compared with the support vector machines (SVM), adaptive neuro-fuzzy inference system (ANFIS) and hybrid ANFIS-particle swarm optimization (PSO). The results proved that the GPR-squared exponential model with the *R*-square (R^2) of 0.948 can forecast D_{80} better than the SVM with the R^2 of 0.83, ANFIS with the R^2 of 0.81 and ANFIS-PSO with the R^2 of 0.89.

Keywords Blasting · Rock fragmentation · Gaussian process regression · Predictive model

1 Introduction

Blasting is the process of using explosive material to fragment or displace the rock masses. Appropriate particle size distribution is one of the most important aims in mining and tunneling industries. On the other hand, the optimum particle size distribution leads to increase in crusher and mill throughput, increase in loader and excavator productivity as well as decrease in energy consumption in size reduction process [1–3]. According to the mentioned descriptions, accurate predictions of rock fragmentation are a necessary work in this field, especially to optimize the overall mine/plant economics. In the literature, many parameters such as blast design parameters are considered as the effective parameters on fragmentation [4–6]. Burden, spacing, stemming, sub-drilling, number of blast-holes, number of rows in blasting pattern, height benches, blast-holes depth, delay times between rows, type of explosives such as ANFO and dynamite, weight used charge per delay and powder factor are all blast design parameters. In recent years, the use of soft computing methods has been widely used for solving different engineering problems [7–13]. In the field of rock fragmentation prediction, several soft computing methods have been proposed by researchers. Artificial

✉ Wei Gao
gaowei@ynnu.edu.cn

Masoud Karbasi
m.karbasi@znu.ac.ir

Mahdi Hasanipanah
Hasanipanah.m@gmail.com

Xun Zhang
zhangxun@swu.edu.cn

Jia Guo
soap_jia@126.com

1 School of Information Science and Technology, Yunnan Normal University, Kunming 650500, China

2 Water Engineering Department, Faculty of Agriculture, University of Zanjan, Zanjan, Iran

3 Young Researchers and Elite Club, Qom Branch, Islamic Azad University, Qom, Iran

4 Department of Editorial, Southwest University, Chongqing 400715, China

5 Department of Engineering, Information Engineering University, Zhengzhou 450001, China

neural networks (ANN) and multiple regression (MR) were employed by Monjezi et al. [5] for predicting the rock fragmentation using five input parameters, i.e. burden to spacing ratio, weight used charge per delay, stemming and blastholes depth. Based on their obtained results, ANN was a suitable method for forecasting the rock fragmentation and its results were more accurate than the MR results. Xiuzhi et al. [1] employed the support vector machines (SVM), ANN, MR for the estimation of rock fragmentation. Their results showed significant capability of the SVM compared to ANN and MR in forecasting rock fragmentation. In the other study of soft computing methods, Monjezi et al. [4] offered the use of fuzzy inference system (FIS) for predicting the rock fragmentation, so that burden, spacing, weight used charge per delay, stemming, powder factor and rock density were adopted as the input parameters. They showed that the accuracy of FIS was superior to that of MR. A comprehensive research work was carried out for forecasting the rock fragmentation in Chadormalu iron mine, Iran, by Esmaeili et al. [14] based on adaptive neuro-fuzzy inference system (ANFIS), SVM and Kuz-Ram empirical model. Respectively, the amount of *R*-square (R^2) for the ANFIS, SVM and Kuz-Ram empirical models were obtained as 0.89, 0.83 and 0.38. These values indicate that the performance capacity of ANFIS is better than SVM and Kuz-Ram empirical models. Recently, Hasanipanah et al. [6] offered the use of a hybrid model of ANFIS-optimized by particle swarm optimization (PSO) for predicting the rock fragmentation. For comparison aims, ANFIS, SVM and MR models were also employed in their study. Their results indicated that the ANFIS-PSO possessed superior predictive ability than the ANFIS, SVM and MR models, since a very close agreement between the measured and the predicted values was obtained. The main objective of the present research is to investigate the ability of Gaussian process regression (GPR) for forecasting the rock fragmentation in the Shur river dam region, Iran.

2 Case study

In the present research work, the blast database is taken from Hasanipanah et al.'s [6] results compiled in Shur river dam area, Iran. Shur river dam is the tallest asphaltic concrete core dam in Iran, located in Kerman Province and near to Sarcheshmeh copper mine. This dam has 85.5 m height from the foundation and the crest length is 450 m. To construct the Shur river dam, two mines were extracted in the around area using bench blasting method. In blasting process, ANFO was utilized as the explosive material for charging the drilled holes. Afterwards, the holes were stemmed using fine gravels. As mentioned in the introduction, an appropriate particle size distribution after mine blasting is one of the most important aims in mining process. Also, accurate predictions of rock fragmentation are a necessary work to optimize the overall mine/plant economics. To achieve these aims, a comprehensive research work was carried out for forecasting the rock fragmentation. In this regard, a database including 72 datasets was prepared, so that the values of burden, spacing, stemming, weight used charge per delay and powder factor, as the effective parameters on fragmentation, were measured. The quality of fragmentation has been also evaluated on the basis of 80% passing size (D_{80}) using image processing method. For image analysis, a digital camera was used and the images were analyzed by using Split Desktop software. For instance, a sample size distribution curve obtained through the Split Desktop is shown in Fig. 1. More details regarding measured datasets are also given in Table 1. To develop the predictive models, the datasets were divided into the following two sets: (1) training datasets. This is applied to build the predictive models. In this research, 58 datasets were assigned as the training datasets; (2) testing datasets. This is applied to test the built predictive

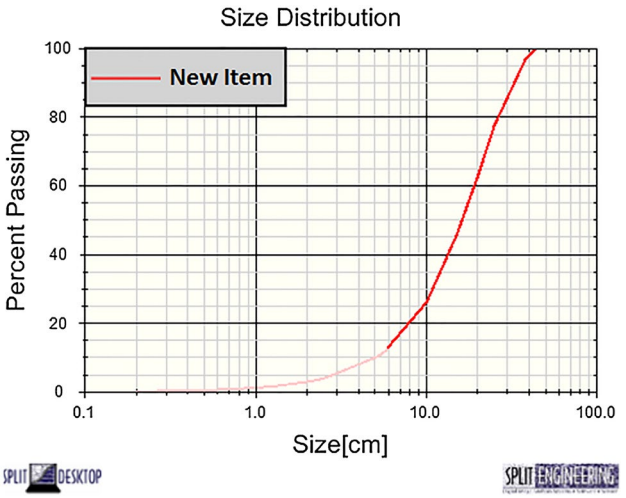

Fig. 1 Sample of a size distribution curve obtained using Split Desktop software

Table 1 The used parameters in this research for the D_{80} estimation

Type of data	Symbol	Range		Mean
		Min	Max	
Input	B (m)	2.7	4.1	3.5
	S (m)	3.4	5.3	4.4
	ST (m)	1.8	3.4	2.7
	PF (g/cm^3)	152	214	179.2
	W (kg)	735	2110	1349.4
Output	D_{80} (cm)	13	42	24.9
No. of samples	72			

B burden, *S* spacing, S_T stemming, *W* weight used charge per delay, *PF* powder factor

models. The remaining 14 datasets were assigned as the testing datasets. Table 2 summarizes the basic statistics of the train and test sets.

3 Gaussian process regression (GPR)

In the present study, GPR is proposed for forecasting the D_{80}. A Gaussian process (GP) is a probabilistic nonparametric model, where observations occur in a continuous domain [15]. It can be used for solving non-linear regression [16] and classification [17] problems. A GPR directly defines a prior probability distribution over a latent function. GPR is specified by its mean function and covariance (kernel) function.

$$f(\mathbf{x}) \sim GP(m(\mathbf{x}),\ k(\mathbf{x}, \mathbf{x}')). \tag{1}$$

The mean function is often assumed zero, as it encodes central tendency of the function [18]. The covariance function encodes information about shape and structure of the function that we expect to have. The connection among input and output variables is expressed as:

$$y = f(\mathbf{x}) + \ \varepsilon. \tag{2}$$

It is assumed that noise ε is independent and a Gaussian distribution with zero mean and σ_n^2 variance is distributed over it.

$$\varepsilon \sim \mathcal{N}\ (0,\ \sigma_n^2). \tag{3}$$

According to Eq. (2), the likelihood is given by

$$p(\mathbf{y}|\boldsymbol{f}) = \mathcal{N}(\mathbf{y}|\boldsymbol{f},\ \sigma_n^2 I\ ), \tag{4}$$

where $\mathbf{y} = [y_1,\ y_2, \ldots,\ y_n]^T, \boldsymbol{f} = [f(\mathbf{x}_1), f(\mathbf{x}_2), \ldots,\ f(\mathbf{x}_3)]$ and I is a $M \times M$ unit matrix.

According to the definition of Gaussian process [19], the marginal distribution $p(\boldsymbol{f})$ is given by a Gaussian whose mean is zero and whose covariance is defined by a Gram matrix, so that

$$p(\boldsymbol{f}) = \mathcal{N}(\boldsymbol{f}|0,\ K), \tag{5}$$

where $K = k(x_i,\ x_j)$. Since both Eqs. (4) and (5) follow the Gaussian distribution, the marginal distribution of y is given by

$$p(\mathbf{y}) = \int p(\mathbf{y}|\boldsymbol{f})p(\boldsymbol{f})\mathrm{d}\boldsymbol{f} = \mathcal{N}(\boldsymbol{f}|0, K_y), \tag{6}$$

where $K_y = K + \sigma_n^2 I$.

To predict the target variable y_* for a new input ($\mathbf{x}_*$), the joint distribution over $y_1, y_2, \ldots, y_m, y_*$ is given by

$$\begin{bmatrix} y \\ y_* \end{bmatrix} = \left(\begin{bmatrix} f \\ f_* \end{bmatrix} + \begin{bmatrix} \varepsilon \\ \varepsilon_* \end{bmatrix} \right) \sim \mathcal{N}\left(0,\ \begin{bmatrix} K_y & \mathbf{k}_* \\ \mathbf{k}_*^T & k_{**} + \sigma_n^2 \end{bmatrix} \right), \tag{7}$$

where $f_* = f(\mathbf{x}_*)$ is the latent function for input variable $\mathbf{x}_*$ and ε_* is corresponding noise; $\mathbf{k}_* = \left[k(\mathbf{x}_*, \mathbf{x}_1), \ldots,\ k(\mathbf{x}_*, \mathbf{x}_M)\right]^T$ and $k_{**} = k(\mathbf{x}_*, \mathbf{x}_*)$. Using the rules for conditioning Gaussians [20], the predictive distribution $p(y_*|\mathbf{y})$ is a Gaussian distribution with mean and covariance given by

$$m(x_*) = \mathbf{k}_*^T K_y^{-1} \mathbf{y}, \tag{8}$$

$$\sigma^2(\mathbf{x}_*) = k_{**} - \mathbf{k}_*^T K_y^{-1} \mathbf{k}_* + \sigma_n^2. \tag{9}$$

The Cholesky decomposition [21] can be used to calculate the inverse of the covariance matrix K_y. The covariance (kernel) function is a critical component in a Gaussian process regression. In supervised learning, similarity among data is very important. The covariance function defines this similarity [21]. In this research, the following covariance function was used:

- Squared Exponential Kernel

$$k(x_i,\ x_j|\theta) = \ \sigma_f^2 \exp\left[-\frac{1}{2} \frac{(x_i - x_j)^T (x_i - x_j)}{\sigma_l^2} \right]. \tag{10}$$

- Exponential Kernel

$$k(x_i,\ x_j|\theta) = \ \sigma_f^2 \exp\left[-\frac{r}{\sigma_l} \right]. \tag{11}$$

- Matern 3/2

$$k(x_i,\ x_j|\theta) = \ \sigma_f^2 \left(1 + \frac{\sqrt{3}\, r}{\sigma_l} \right) \exp\left[-\frac{\sqrt{3}\, r}{\sigma_l} \right]. \tag{12}$$

Table 2 The basic statistics of the train and test sets in the present study

	No. of samples	Parameters	Min	Mean	Max
Train set	58	B (m)	2.8	3.5	4.1
		S (m)	3.4	4.4	5.3
		S_T (m)	1.8	2.7	3.4
		W (kg)	735	1345	2210
		PF (g/cm^3)	152	179	214
		D_{80} (cm)	13	25.3	42
Test set	14	B (m)	2.7	3.4	4.1
		S (m)	3.5	4.4	5.3
		S_T (m)	2	2.8	3.4
		W (kg)	940	1367.5	1945
		PF (g/cm^3)	158	180	201
		D_{80} (cm)	18	23.6	31

- Matern 5/2

$$k(x_i,\ x_j|\theta) = \sigma_f^2\left(1+\frac{\sqrt{5}\,r}{\sigma_l}+\frac{5r^2}{3\sigma_l^2}\right)\exp\left[-\frac{\sqrt{5}\,r}{\sigma_l}\right]. \quad (13)$$

- Rational Quadratic Kernel

$$k(x_i,\ x_j|\theta) = \sigma_f^2\left(1+\frac{r^2}{2\alpha\sigma_l^2}\right)^{-\alpha}, \quad (14)$$

where $r=\sqrt{(x_i-x_j)^T(x_i-x_j)}$ is the Euclidean distance between x_i and x_j, σ_l is the characteristic length scale and σ_f is the signal standard deviation. Hyperparameters of the covariance function $\theta(\sigma_l\ ,\ \sigma_f)$ can be estimated from the above equations using a gradient-based algorithm [21]. The performance capacity of the Squared Exponential Kernel, Exponential Kernel, Matern 3/2, Matern 5/2 and Rational Quadratic Kernel models in predicting the D_{80} is evaluated in the next section.

4 Results and discussion

In the present research work, various GPR models, i.e. Squared Exponential Kernel, Exponential Kernel, Matern 3/2, Matern 5/2 and Rational Quadratic Kernel models have been employed for forecasting the D_{80}. The predicted D_{80} values by the GPR models are summarized in Table 3. To evaluate the proposed models performance, the following expressions were used:

$$\mathrm{RMSE} = \sqrt{\frac{\sum_{i=1}^{N}(O_i-P_i)^2}{N}}, \quad (15)$$

$$\mathrm{RRMSE} = \frac{\mathrm{RMSE}}{\bar{O}_i}, \quad (16)$$

$$\mathrm{MBE} = \frac{1}{N}\sum_{i=1}^{N}(O_i-P_i), \quad (17)$$

$$\mathrm{MAPE} = \frac{1}{N}\sum_{i=1}^{N}\left|\frac{O_i-P_i}{O_i}\right|, \quad (18)$$

$$R^2 = \frac{\left(\sum_{i=1}^{N}(O_i-\bar{O}_i)(P_i-\bar{P}_i)\right)^2}{\sum_{i=1}^{N}(O_i-\bar{O}_i)^2\sum_{i=1}^{N}(P_i-\bar{P}_i)^2}, \quad (19)$$

where O_i is the actual value, P_i is the predicted value, $\bar{O}_i$ is the mean value of actuals, $\bar{P}_i$ is the mean value of predictions, i is the subscript which indicates the ID of data, and N is the total number of data. The RMSE describes the average difference between predicted value and measured value. The mean average error (MBE) shows how models overestimate or underestimate the measured values. The mean average percentage error (MAPE) describes the accuracy of the

Table 3 Comparison between the actual D_{80} vs. the predicted values for testing datasets

No. of data	Actual D_{80} (cm)	Measured D_{80} (cm)				
		Squared Exponential Kernel	Exponential Kernel	Matern 3/2	Matern 5/2	Rational Quadratic Kernel
1	21	20.33	20.63	20.63	20.63	19.71
2	19	21.88	22.43	22.43	22.43	21.80
3	14	17.54	17.59	17.59	17.59	17.96
4	15	16.14	16.17	16.17	16.17	16.27
5	31	30.76	30.83	30.83	30.83	29.80
6	34	33.30	32.87	33.12	33.28	33.33
7	19	18.41	18.28	18.28	18.28	19.38
8	33	33.80	33.70	33.70	33.70	34.39
9	28	29.67	29.66	29.66	29.66	29.95
10	31	32.68	32.60	32.60	32.60	33.65
11	31	31.49	31.49	31.49	31.49	31.39
12	21	25.93	25.96	25.96	25.96	25.45
13	35	34.65	33.63	33.81	33.94	33.82
14	24	25.47	25.59	25.59	25.59	25.93

Table 4 The values of RMSE, RRMSE, MBE, MAPE and R^2 for the various GPR models using testing datasets

Model	Kernel type	RMSE	R^2	MBE	MAPE (%)	RRMSE (%)
GPR	Squared exponential	2.01	0.948	1.14	7.36	7.90
GPR	Exponential	2.12	0.939	1.10	7.84	8.34
GPR	Matern32	2.10	0.942	1.13	7.75	8.26
GPR	Matern52	2.09	0.943	1.15	7.69	8.22
GPR	Rational quadratic	2.18	0.936	1.20	8.50	8.58

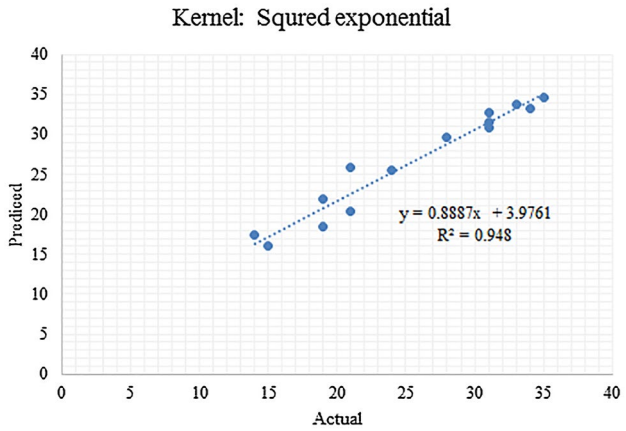

Fig. 2 The performance of the squared exponential model for forecasting the D_{80}

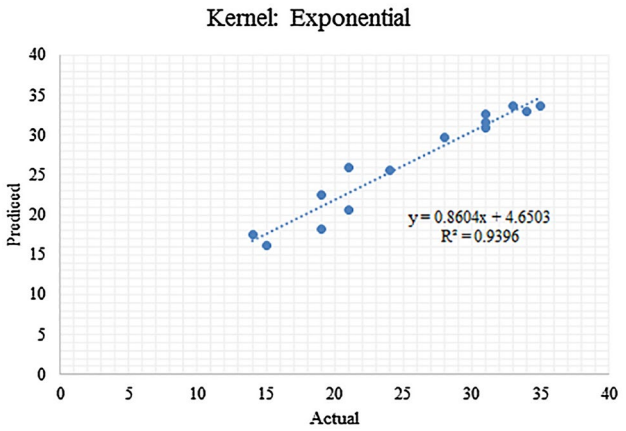

Fig. 3 The performance of the exponential kernel model for forecasting the D_{80}

models by error percentage. The coefficient of determination R^2 describes the degree of association between the predicted and the measured values. The performance of the model according to RRMSE is defined as follows [22]:

Excellent if: RRMSE < 10%

Good if: 10% <RRMSE < 20%

Fair if: 20% <RRMSE < 30%

Poor if: RRMSE > 30%

The values of the mentioned expressions obtained from the predictive models are given in Table 4. Moreover, Figs. 2, 3, 4, 5 and 6 illustrate the scatter plots of D_{80} predicted by the models for only testing datasets. As shown in Table 4 and Figs. 2, 3, 4, 5 and 6, the predicted values using the developed GPR models are in good agreement with the actual data, which demonstrates the reliability of the GPR models for forecasting the D_{80}. The amount of R^2 for the Squared Exponential Kernel, Exponential Kernel, Matern 3/2, Matern 5/2 and Rational Quadratic Kernel models was obtained as 0.948, 0.939, 0.942, 0.943 and 0.936, respectively. These values indicate that the performance capacity of GPR-Squared Exponential model is better than the other models. It should be mentioned that the used datasets in this research were already used by Hasanipanah et al. [6]. In their study, SVM, ANFIS and ANFIS-PSO models were

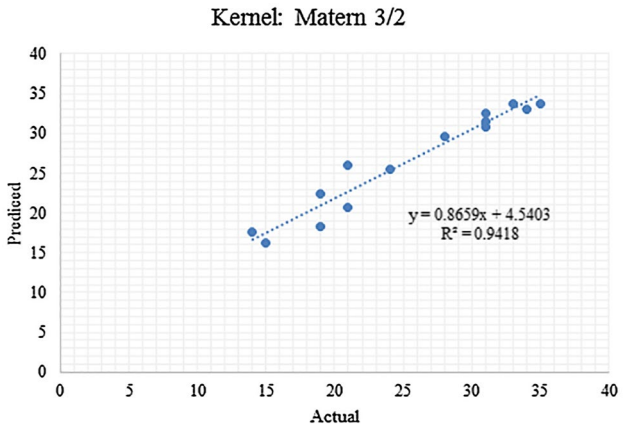

Fig. 4 The performance of the matern 3/2 model for forecasting the D_{80}

employed for forecasting the D_{80}. They concluded that the ANFIS-PSO model with the R^2 of 0.89 for the testing set was a useful model for predicting the D_{80} and its results were more accurate than the SVM and ANFIS models. As shown in Table 4, performance of the developed models by Hasanipanah et al. [6] can be improved to R^2 of 0.948 in the

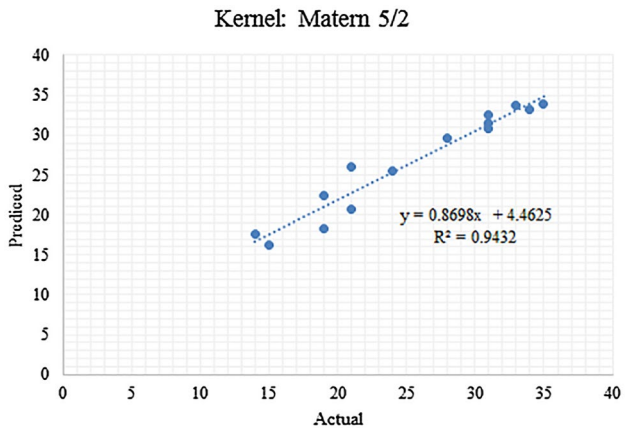

Fig. 5 The performance of the matern 5/2 model for forecasting the D_{80}

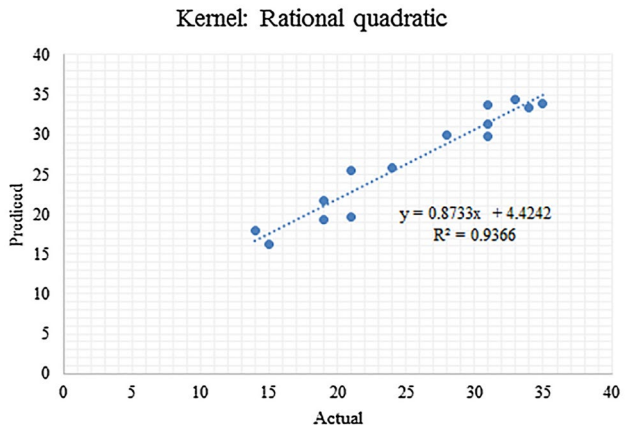

Fig. 6 The performance of the rational quadratic model for forecasting the D_{80}

present study. In other words, the GPR-Squared Exponential model presented in this study is more acceptable model for the D_{80} prediction in comparison to the SVM, ANFIS and other GPR models. In other words, this work presents the applicability of GPR-Squared Exponential model as an estimator and method employed could be useful to forecast the D_{80}. Also, sensitivity analysis is performed in the present study, as shown in Table 5. Based on this table, when the PF was omitted from the modeling process, the performance capacity of GPR-Squared Exponential model was significantly decreased. In other words, the PF was the most effective independent parameter in the GPR-modeling process in the present study.

5 Conclusion

Precise estimation of rock fragmentation is a necessary work to optimize the overall mine/plant economics. In the present study, various types of GPR are proposed for forecasting the rock fragmentation. In this regard, Squared Exponential Kernel, Exponential Kernel, Matern 3/2, Matern 5/2 and Rational Quadratic Kernel were employed and then their performances were compared. For developing the predictive models, 72 datasets were gathered from the Shur river dam region, in Iran, using five independent (input) parameters, i.e. PF, W, S, B and S_T as well as one dependent parameter (output), namely D_{80}. Firstly, 58 datasets were used for constructing the predictive models and then the remaining 14 datasets were used to test the models. The performance capacity of the GPR models was evaluated based on several statistical functions, i.e. RMSE, RRMSE, MAPE, MBE and R^2. Based on the obtained results, the accuracy of the GPR-squared exponential model was higher than the other GPR models in predicting the D_{80}. It is important to note that the datasets used in this study were already utilized by Hasanipanah et al. [6]. In their study, SVM, ANFIS and PSO-ANFIS models were offered for forecasting the D_{80}. Hence, we can compare the predicted values by the GPR models with the Hasanipanah et al.'s [6] results. Finally, it was found that the GPR-Squared Exponential model with $R^2 = 0.948$ has better performance than the GPR-Exponential Kernel with $R^2 = 0.939$, the GPR-Matern 3/2 with $R^2 = 0.942$, the GPR-Matern 5/2 with $R^2 = 0.943$, the GPR-Rational Quadratic Kernel with $R^2 = 0.936$, the ANFIS with $R^2 = 0.81$, the SVM with $R^2 = 0.83$ and the ANFIS-PSO with $R^2 = 0.89$. In addition, the sensitivity analysis was carried out and based on the obtained results, PF was chosen as the most effective factor on the D_{80} in the present study.

Table 5 The results of sensitivity analysis for selecting the most effective parameter on D_{80}

Model	Omitted	RMSE	R^2	MBE	MAPE (%)	RRMSE (%)
GPR	B	2.01	0.948	1.14	7.36	7.88
GPR	PF	3.82	0.704	−0.25	12.05	15.03
GPR	S	2.14	0.936	1.16	7.99	8.41
GPR	S_T	2.13	0.944	1.26	7.82	8.38
GPR	W	3.27	0.862	1.59	13.04	12.86

References

1. Shi XZ, Zhou J, Wu B, Huang D, Wei W (2012) Support vector machines approach to mean particle size of rock fragmentation due to bench blasting prediction. Trans Nonferrous Met Soc China 22:432–441
2. Ebrahimi E, Monjezi M, Khalesi MR, Armaghani DJ (2015) Prediction and optimization of back-break and rock fragmentation using an artificial neural network and a bee colony algorithm. Bull Eng Geol Environ. https://doi.org/10.1007/s10064-015-0720-2
3. Trivedi R, Singh TN, Raina AK (2016) Simultaneous prediction of blast-induced flyrock and fragmentation in opencast limestone mines using back propagation neural network. Int J Min Miner Eng 7(3):237–252
4. Monjezi M, Rezaei M, Yazdian Varjani A (2009) Prediction of rock fragmentation due to blasting in Gol-E-Gohar iron mine using fuzzy logic. Int J Rock Mech Min Sci 46:1273–1280
5. Monjezi M, Bahrami A, Yazdian Varjani A (2010) Simultaneous prediction of fragmentation and flyrock in blasting operation using artificial neural networks. Int J Rock Mech Min Sci 47(3):476–480
6. Hasanipanah M, Bakhshandeh Amnieh H, Arab H, Zamzam MS (2016) Feasibility of PSO–ANFIS model to estimate rock fragmentation produced by mine blasting. Neural Comput Appl. https://doi.org/10.1007/s00521-016-2746-1
7. Verma AK, Singh TN (2011) Intelligent systems for ground vibration measurement: a comparative study. Eng Comput 27(3):225–233
8. Verma AK, Singh TN (2013) A neuro-fuzzy approach for prediction of longitudinal wave velocity. Neural Comput Appl 22(7–8):1685–1693
9. Verma AK, Singh TN, Chauhan NK, Sarkar K (2016) A hybrid FEM–ANN approach for slope instability prediction. J Inst Eng (India) Ser A 97(3):171–180
10. Singh J, Verma AK, Banka H, Singh TN, Maheshwar S (2016) A study of soft computing models for prediction of longitudinal wave velocity. Arab J Geosci 9(3):1–11
11. Gao W, Farahani MR, Aslam A, Hosamani S (2017) Distance learning techniques for ontology similarity measuring and ontology mapping. Cluster Comput J Netw Softw Tools Appl 20(2):959–968
12. Gao W, Farahani MR (2017) Generalization bounds and uniform bounds for multi-dividing ontology algorithms with convex ontology loss function. Comput J 60(9):1289–1299
13. Gao W, Baig AQ, Ali H, Sajjad W, Farahani MR (2017) Margin based ontology sparse vector learning algorithm and applied in biology science. Saudi J Biol Sci 24(1):132–138
14. Esmaeili M, Salimi A, Drebenstedt C, Abbaszadeh M, Aghajani Bazzazi A (2014) Application of PCA, SVR, and ANFIS for modeling of rock fragmentation. Arab J Geosci. https://doi.org/10.1007/s12517-014-1677-3
15. Grbić R, Kurtagić D, Slišković D (2013) Stream water temperature prediction based on Gaussian process regression. Expert Syst Appl 40(18):7407–7414
16. Williams CKI (1997) Regression with Gaussian processes. In: Ellacott SW, Mason JC, Anderson IJ (eds) Mathematics of neural networks: models, algorithms and applications. Operations Research/Computer Science Interfaces Series No. 8. Kluwer, pp 378–382
17. Williams CKI, Barber D (1998) Bayesian classification with Gaussian processes. IEEE Trans Pattern Anal Mach Intell 20(12):1342–1351
18. Zhang C, Wei H, Zhao X, Liu T, Zhang K (2016) A Gaussian process regression based hybrid approach for short-term wind speed prediction. Energy Convers Manag 126:1084–1092
19. MacKay DJ (1998) Introduction to Gaussian processes. NATO ASI Series F Comput Syst Sci 168:133–166
20. Bishop CM (2006) Pattern recognition. Mach Learn 128:1–58
21. Rasmussen CE, Williams CKI (2006) Gaussian processes for machine learning, vol 38. The MIT Press, Cambridge, pp 715–719
22. Mihoub R, Chabour N, Guermoui M (2016) Modeling soil temperature based on Gaussian process regression in a semi-arid-climate, case study Ghardaia, Algeria. Geomechanics and Geophysics for. Geo Energy Geo Resour 2(4):397–403. https://doi.org/10.1007/s40948-016-0033-3